



Automatic Optimization of Initial Blank Shape in Production of All Kinds of Rectangular Parts in Computer Aided Hydroforming Process

R. Mousavipoor, H. Gorji*, M. Bakhshi-Jooybari, M. Shakeri

Department of Mechanics, Faculty of Mechanical Engineering, Noshirvani University of Technology, Babol, Iran

PAPER INFO

Paper history:

Received 30 July 2023

Received in revised form 26 October 2023

Accepted 27 October 2023

Keywords:

Deep Drawing

Automatic Optimization

Blank Optimization

Blank Automation Flowchart

ABSTRACT

In this research, an innovative method has been applied to obtain the shape of initial sheet in the forming of different rectangular geometries. So that we can define rules that automatically determine the optimal shape of the initial sheet at different heights. Sensitivity analysis method was used for optimization, and Python software was used to link with Abaqus software. By examining the geometrical parameters and forming pressure, a flowchart was presented to determine the appropriate pressure. By examining the height changes in different geometries, it was found that the optimization reduces the maximum pressure and the maximum radius of the punch, which were obtained by 4 and 8%, respectively. It was found that the difference in the size of the longitudinal and transverse sides of the section has a direct effect on the changes in the node coordinates to plot the target curve and reduces the number of optimization steps. According to the results, it was shown that by automation and determining the pressure flowchart, the shape of the initial sheet can be determined without repeating the optimization stages and experimental tests. It also prevents material waste.

doi: 10.5829/ije.2024.37.04a.09

1. INTRODUCTION

Non-circular parts, particularly those with square and rectangular geometries, are widely used in industry to manufacture main parts in the car body, fuel system components, oil tanks, main components of aircrafts, etc. The production of rectangular and polygonal sheet metal parts is recognized as a complicated activity in industry. The primary method employed for manufacturing such products is metal stamping. However, in traditional processes, achieving consistent production quality with uniform thickness distribution is difficult due to the complexity of the geometries involved. Moreover, several forming stages are required. In certain cases, these parts may feature multiple steps or polyhedral geometries, with sharp corners present at the intersections of these steps or within the part walls. The intricate nature of these features, along with the inherent challenges of material flow in such regions, make it difficult to form the parts by traditional methods such as stamping. By using new methods in production of difficult-to-form sheet parts,

more uniform thickness distribution and higher quality can be achieved.

Sheet hydroforming is a modern sheet metal forming processes that has been used in production of car parts and aircraft bodies since 1980s (1). This process has grown increasingly in recent years in the industry, especially in automobile manufacturing (2). Hydroforming has several advantages such as higher forming limit, better surface quality, higher tensile strength, and higher dimensional accuracy (3, 4). In this process, some preforms may be needed to achieve the proper final shape of the workpiece without defects and excessive material waste (5). Among the various effective parameters in sheet forming processes, the initial shape of the sheet plays a vital role, as optimizing it can significantly impact the production of parts with minimal cost and high quality. Moreover, the optimization of the initial blank increases the drawing ratio, reduces the sheet consumption, and reduces the number of production stages. However, it is very difficult to determine the optimum shape of the initial blank due to the complexity of the material behavior, especially in

*Corresponding Author Email: hamidgorji@nit.ac.ir (H. Gorji)

stamping and deep drawing processes in which complicated deformation mechanics are involved.

Currently, according to the different methods provided by researchers, the optimization methods can be divided into two categories: retro-marching and iterative design (6). Slip line field method (7), geometric mapping method (8), area addition and subtraction method (9), inverse finite element method (10), ideal deformation theory (11) and backward finite element tracking (12) are among the methods belong to the retro-marching plan. However, since in this category it is not possible to compensate the shape error which refer to the difference between the desired final shape and the deformed shape, by using finite element analysis (obtained from the predicted initial shape), the mentioned methods provide limited accuracy. But, in iterative designs, the initial shape is guessed and is frequently corrected by considering the shape error until the deformed shape matches the desired final shape. The sensitivity method (13), and the radius vector method (9) belong to this category.

Since the above-mentioned categories provide excellent accuracy and good convergence, they can be used to predict the optimum blank with complicated shapes in processes such as stamping and deep drawing. The methods of sensitivity analysis and radius vector are more useful in each process due to the ease of determining the changes in nodes coordinates and the ability to generalize the relationships based on new parameters. According to the flowchart of the sensitivity analysis method, after determining the target curve related to the flange area, a blank is guessed, the simulation is done, and at the end of the forming process, the amount of deviation of all the nodes from the target curve is obtained (6).

According to the various ranges of commonly used geometries for rectangular parts, stepped geometries are of special importance. Depending on their specific application, these parts can be categorized as side-step parts, middle-step parts, or parts with multiple steps. In all of these cases, due to the existence of the intersections between the steps and the importance of producing a workpiece with complete filling, optimizing the initial dimensions of the sheet can be very important, because it makes it easier for the sheet to flow in the corners, decreases the forming pressure, and reduces the production time.

Research efforts focused on the automatic optimization of the blank shape for all types of parts with a rectangular section have been relatively scarce. Meng et al. (14) investigated the effect of fluid pressure in hydroforming a rectangular aluminum workpiece. They found that the hydroforming process improves the quality of the parts. They also stated that by increasing the fluid pressure, the formability of the part improves. Rahmani et al. (15) investigated the effective parameters in the forming of parts with square sections. These researchers investigated the possibility of achieving the maximum

drawing ratio by considering the effect of pressure parameters, sheet thickness, and friction coefficient. They found that with an increase in friction coefficient, the range of the drawing ratio is limited due to the decrease in the flow of the sheet. Moreover, as the thickness of the sheet increases, a higher drawing ratio is obtained. Mousavipoor et al. (16) investigated the feasibility of forming two-step rectangular parts in a single stage and optimized the dimensions of the blank with experimental investigation and simulation. They found that the effect of forming pressure on the thickness distribution of the part depends on the shape of the product and the type of the hydroforming process. By examining the amount of die filling, they concluded that to achieve complete die filling, the fluid pressure should be increased throughout the process. They also stated that optimization of the sheet blank leads to improve the material flow and a more uniform thickness distribution. Luo et al. (17) presented a new method for forming a rectangular workpiece using a mechanical preforming operation, which was a combination of deep drawing process and superplastic forming. In this research, three different metals have been used: aluminum SPF 5083 with super-plasticity properties, aluminum AA5183, which does not have super-plasticity properties, and AZ31 without super-plasticity properties. The second and third metals were fine-grained through rolling. By comparing the two forming modes with the Hot Draw Mechanical Preforming (HDMP) process and superplastic forming with the obtained pressure curve, it was found that the time of the superplastic forming was longer than that of HDMP. On the other hand, the amount of pressure required in the superplastic forming was lower. Finally, the parts produced using the superplastic forming had rupture in the corners. This was due to the use of the two stages of preforming and final forming, and the control of the strains created in the mentioned combined process. Then, the effects of different parameters on the thickness distribution of the part have been investigated. The results showed that by increasing the diameter of the punch and the drawing depth, the thickness decreases. Vafaesefat (18) examined the optimization of the blank shape for the two geometries of square cup and oil pan drawings made of St14 by using the iterative finite element method. By considering the first square geometry in the analysis, an error occurred due to the lack of sheet flow. Next, by performing iterative finite element analysis, the contours of the target and the formed workpiece coincided with the shape error of 0.9435 mm, the optimum sheet shape was obtained, and the final part was formed. Blount and Fischer (19) investigated the earing phenomenon of aluminum alloy 2048 cup-shaped parts. Using an algorithm, they first simulated the process. After specifying the target curve, the amount of deviation of each node from the target curve was obtained and the average of these values were recorded as an error. Then,

using a coefficient whose value was chosen arbitrarily, the position of each node of the undeformed sheet was changed and the simulation was repeated until the error value was less than the desired value.

In recent years, extensive research has been conducted on various optimization methods for sheet metal parts. However, due to the diverse range of geometries of industrial sheet parts and the variations in drawing depths and final workpiece dimensions, there is a lack of a comprehensive design guide or general relationship to determine the dimensions of the initial sheet for each geometry. Furthermore, manual optimization methods need to be applied separately for circular and rectangular geometries at different depths.

As a result, there is currently no universally applicable method or rule for extracting the initial blank shape for any given geometry. Consequently, there is a need for a method that can automatically establish rules for optimizing the dimensions of the initial sheet by utilizing coding and establishing links between analytical and simulation software. Such a method, with a focus on classifying rectangular geometries, would prove highly beneficial in the industry.

The key figure in this research is that at first, by classifying a group of rectangular workpieces with varying geometries and depths, the initial sheet dimensions are optimized manually and the procedure of changing the nodes coordinates is investigated. Additionally, by checking the parameters and developing a flowchart to determine the proper pressure, by linking Abaqus, Python and MATLAB software and the basic relations of sensitivity analysis, a method is proposed through which, by coding between the software, for any geometry with different depths and dimensions, the initial sheet shape can be extracted automatically. In this research, the sensitivity method is adopted for optimizing the initial sheet shape. This method is chosen due to its practicality and suitability for automation. Moreover, changes in the shape of the initial blank are evaluated based on the alterations in the coordinates of the nodes. The sensitivity method offers a more practical and user-friendly alternative, particularly for the automated optimization of sheet metal parts. In contrast, other optimization methods are parametric and more complex in terms of defining rules and extracting relationships between variables.

2. DEFINITION OF PART AND DIE GEOMETRY

To ensure a comprehensive investigation of various rectangular geometries, this research initially focuses on simple rectangular and symmetric stepped geometries. Figure 1 illustrates the geometries employed in the study. The maximum depth of the step for two-step parts is considered in the first stage, which can be formed in a

single hydroforming process. Based on Figure 1, the depth of the first step is 10 and 17 mm, while the depth of the lower step is 20 and 13 mm for the middle-step part and the side-step part, respectively.

3. EXPERIMENTAL AND SIMULATION PROCEDURE

The sheet hydroforming process has been modelled using the ABAQUS/Explicit 6-13 software. Due to the symmetry of the defined geometries, only half of the sheet and die components have been 3D modeled. Because of the type of the process and the large deformation of the material, dynamic explicit solution has been employed (20). In the section properties of the software, physical and mechanical properties have been defined for the sheet. Figure 2 shows how to deploy the components of the simulation setup. The contact characteristic used in this research is direct contact. Surface-to-Surface contact is used to define the contacts. Coulomb friction model was used to define the characteristics of the surfaces in contact.

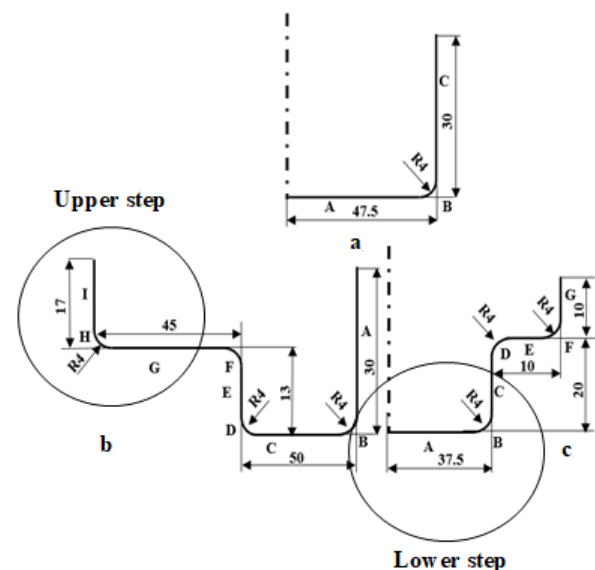


Figure 1. Defined geometries, a. Simple workpiece, b. Side-step workpiece, c. Middle-step workpiece

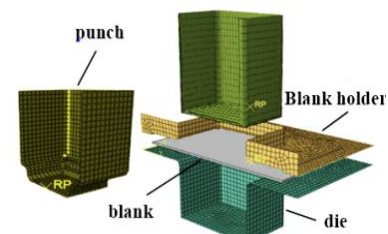


Figure 2. Arrangement of the die setup components in Abaqus

According to Zhang et al. (10), the friction coefficient between the punch and the blank is set to 0.14 and that between the blank with the blank holder and the die is considered to be 0.04.

In conducting the tests, a universal testing machine with a capacity of 600 kN, controlled by a computer, was used. Figure 3 shows the manufactured die components. The characteristics and properties of the steel sheet are listed in Table 1. Figure 4 shows the stress-strain diagram of the sheet obtained from the uniaxial tension test. To investigate the anisotropy properties of the sheet material, samples were prepared and tested in the orientations of 0, 45 and 90 degrees to the rolling direction. Due to the insignificant difference of the obtained coefficients, the sheet was considered isotropic. To obtain the optimum pressure path required for the forming of the defined geometries, the path shown in Figure 5 was considered. To examine the filling in the corners of the die, the filling percentage criterion was used. This criterion is defined as the area swept by the formed sheet to the total area of the die cavity in the critical area (as shown in Figure 6) (21).

Based on the purpose of the paper, which focuses on different geometries with rectangular sections, the initial simulation was conducted using a rectangular geometry with an initial depth (h) of 10 mm. Considering the maximum pressure (according to Figure 5) between 12 and 15 MPa and conducting experiments, a rupture occurred in the punch radius area. Then, by increasing the pressure to 18 MPa, the thinning of the wall led to a

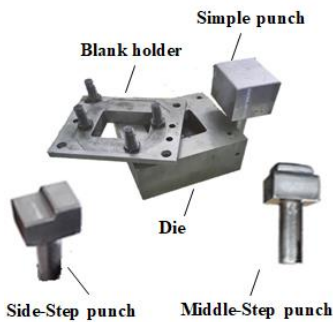


Figure 3. Arrangement of the die setup components in Experimental tests

TABLE 1. Mechanical properties of St13 sheet (10)

Yield strength [MPa]	116
Density [kg/m ³]	$\rho = 8750$
Poisson's ratio	$\nu = 0.33$
Strength constant [Gpa]	$K=180$
Strain hardening exponent	$n=0.44$
Anisotropy parameters	$R0=1, R45=1.018 R90=1.04$
Young's modulus [Gpa]	$E=210$

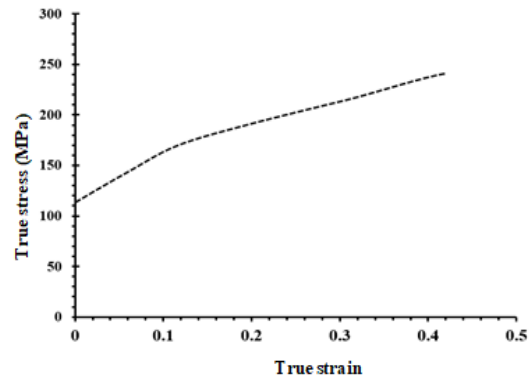


Figure 4. Stress-strain diagram of St13 sheet

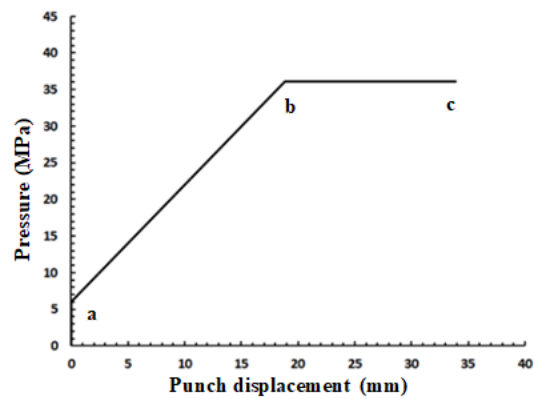


Figure 5. The pressure path used in the research

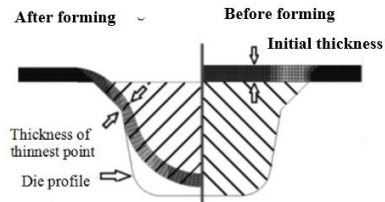


Figure 6. Schematic of determining the percentage of filling in the forming (21)

rupture of the sheet (Figure 7a). Finally, at the pressure of 24 MPa, the sheet material was able to withstand the deformation without rupturing.

To investigate the feasibility of production of stepped parts, by applying the maximum pressure of 24 MPa, it was observed that full filling does not occur in the intersection between the steps. In Figure 7b the rupture and non-filling of the part is shown for the middle-step part at a pressure of 22 MPa. To check the complete forming of the stepped parts, at a depth of 13 mm in the lower step and a maximum pressure of 20 MPa, there is no complete filling in the side-step part and in the middle-step part, and the filling rate is 68 and 60%, respectively. But by increasing the pressure to 40 and 30 MPa, the

filling rate is 84 and 93%, respectively. Finally, by performing the stages of forming stepped parts according to Figure 8, the side-step part was formed and produced at a pressure of 40 MPa. Figure 9 shows the effect of maximum forming pressure of thickness distribution of the deformed part.

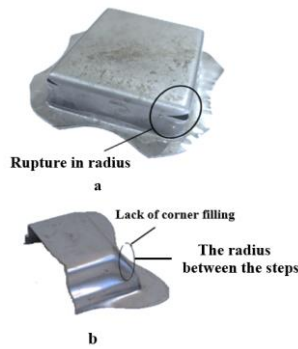


Figure 7. a. Rupture in the punch radius of a simple part at a pressure of 18 MPa, b. Lack of filling in the middle-step part at a pressure of 22 MPa, obtained from simulation



Figure 8. a. Side-step workpiece with a depth of 35 mm and at a pressure of 24 MPa, b. Simple workpiece with a depth of the lower step of 13 mm and at a pressure of 40 MPa, obtained from the experiments

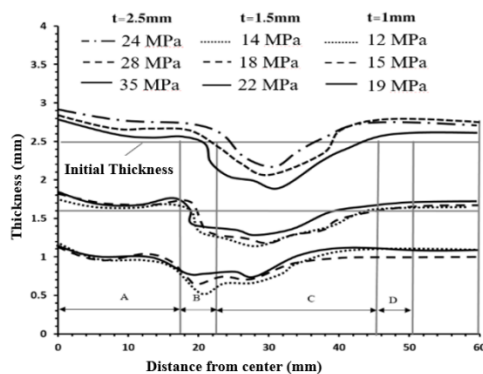


Figure 9. Investigating the effects of maximum fluid pressure on the thickness distribution of a simple workpiece with dimensions of 120 × 130 mm, and thicknesses of 1, 1.5 and 2.5 mm with depth of 35mm, obtained from simulation

According to Figure 9, it was determined that by changing the thickness of the part at a fixed depth, the maximum limit of thickness reduction in the area of the punch radius and the upper wall should be reduced by 5%; for a thickness of 1 mm, it will reach from 32% to 30%, the reason is the reduction of the distance between the critical punch radii from each other and less elongation between the walls. Figure 10 shows the formed parts obtained from the simulations.

4. THE PROPER PRESSURE FLOW CHART

A flowchart is written to obtain the proper pressure for the rectangular parts, which is shown in Figure 11. By coding using Python software and by performing the required simulations in ABAQUS software, the proper pressure value is obtained automatically. Many parameters affect the amount of proper forming pressure. In the flowchart, to obtain the proper pressure for a side-step rectangular workpiece with specific material and thickness, according to Figure 11, at first, the simulation was performed with a pressure of 10 MPa and the amount of thinning created in the part (t_1) was obtained. If the maximum thinning rate decreases with the increase of pressure, increasing the amount of pressure continues. Investigations showed that the increase in pressure to some extent causes the decrease in thickness, and then with the increase of pressure, the thickness reduction increases. If the thickness reduction increases compared to the previous stage, increasing the pressure value is stopped. Therefore, the amount of pressure should be reduced. Through the investigations, it was determined that the suitable pressure for forming is between the n th simulation (P_n) and ($n-1$) th simulation (P_{n-1}). Therefore, the pressure value is reduced with a ratio lower than 5 MPa, so that the pressure change is lower than the previous stage. Now, if increasing the pressure by 5 MPa has caused an increase in thickness reduction for the first time, it happens vice versa (left side of the flowchart). In the flowchart, t_i is the smallest thickness created in the workpiece in each simulation. Using the presented new method, the proper pressure for forming parts a and b was obtained 12 MPa.

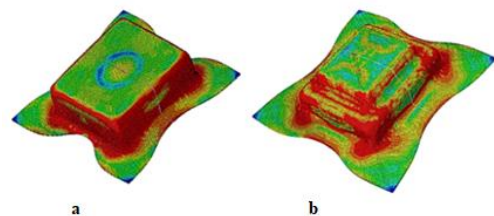


Figure 10. a. Simple part with a depth of 30 mm, a thickness of 2.5 mm, and a maximum pressure of 36 MPa, b. Middle-step part at a depth of 13 mm, a thickness of 2.5 mm, and a maximum pressure of 42 MPa, obtained from simulation

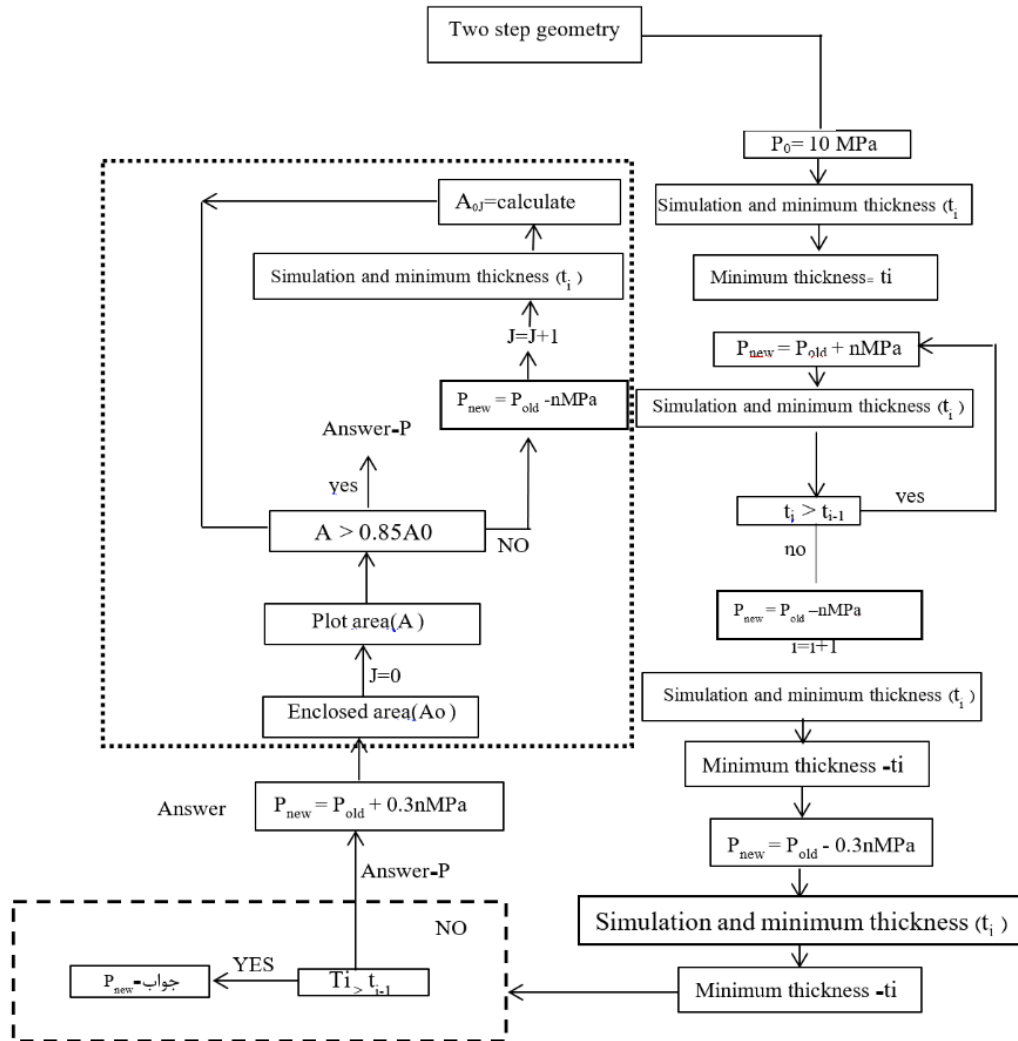


Figure 11. Flowchart of obtaining the proper pressure of a two-step rectangular geometry

5. EFFECT OF FORMING PARAMETERS

5.1. Change in Depth and Drawing Ratio In this research, the process of changing the forming parameters for different geometries is performed, so that the general law of the effects of these parameters can be extracted in the form of a flowchart and be used as initial simulation inputs for each determined geometry. To investigate the effect of step depth on thinning, the forming of rectangular workpieces at depths between 10 and 35 mm was investigated. The depth of the first step for stepped parts was considered from 10 to 20 mm. Figure 12 shows rectangular workpieces at different depths. By examining the same process for the two-step parts (side-step part) as seen in Figure 13, by increasing the step depth, due to the increased strain and elongation experienced during the first step, the thinning in the areas of the wall of the first

step and the radius of the corner of the punch increase. Moreover, it was found that the percentage of thickness reduction at step depths of 10, 13, and 20 mm were 7, 11, and 13 percent, respectively. According to the considered thinning criteria, it is observed that there is no rupture in the workpiece.

5.2. Effect of Punch Radius Due to the variation in drawing ratio, step depth, and the geometry of rectangular parts, the punch corner radius can have a significant impact on the forming process and the resulting thinning behavior of the part. To study this effect for simple and two-step geometries, the radius of 3, 4, 5, and 7 mm were considered. Figure 14a indicates that for the simple part, when the punch corner radius is increased while maintaining a constant pressure, the maximum thinning decreases and the thickness distribution

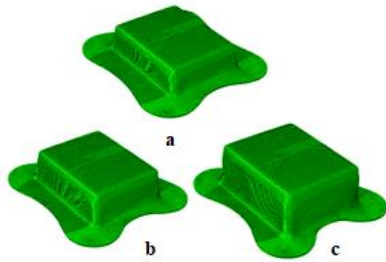


Figure 12. Simple part formed with different step depths at the constant pressure of 24 MPa and a thickness of 1.5 mm, a. Depth of 15 mm, b. Depth of 25 mm, c. Depth of 35 mm, obtained from simulation

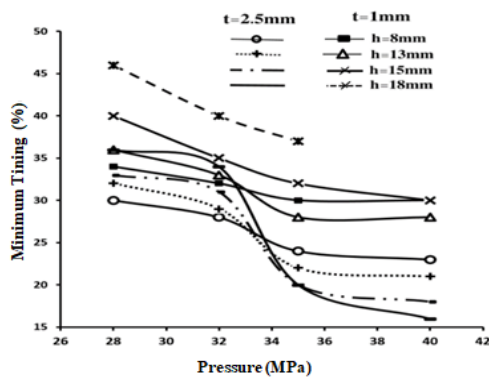


Figure 13. Effect of step depth on thickness distribution in for the side-step part, obtained from simulation

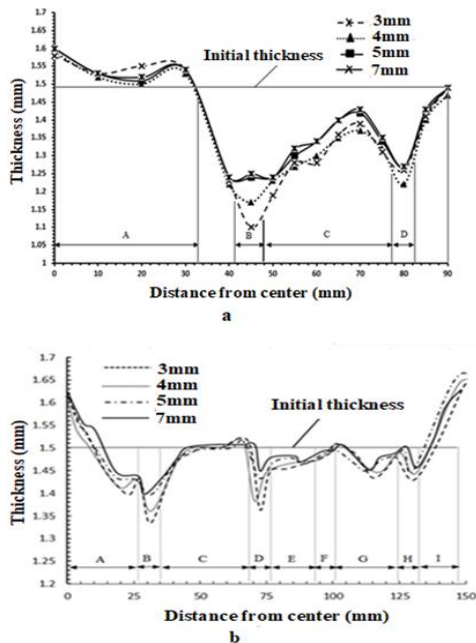


Figure 14. Effect of punch corner radius on thickness distribution, a. Simple workpiece at a pressure of 24 MPa, a depth of 35 mm, and a thickness of 1.5 mm. b. Side-step workpiece at a pressure of 40 MPa, a depth of 13 mm, and a thickness of 1.5 mm, obtained from simulation

improves. By increasing the punch corner radius, bending is reduced, and the material flow is facilitated. It is also observed that at the radii smaller than 3 mm, the percentage of thickness reduction exceeds 42%, as a result, the workpiece is prone to tearing in the punch radius area. It is found that the minimum thickness reduction due to the increase in punch corner radius is 5%. By examining the same process for the two-step parts shown in Figure 14b, it is seen that by increasing the punch corner radius in the lower step area, the process of thickness reduction is similar to that of the simple workpiece. Meanwhile, because of more elongation due to the geometry of the upper step and the intersection of the steps, thinning increases up to 7%. Moreover, rupture in the punch corner radius area in the intersection between the steps is reduced by 4% due to the effect of the fluid pressure in filling the die.

6. OPTIMIZATION

6. 1. Optimization with Sensitivity Method As stated previously, the proper pressure for different geometries has been obtained. In order to examine the process of change of the initial sheet nodes, at first the initial sheet optimization was done manually for three different geometries. To carry out the simulation and experiments, the initial sheet with the dimensions of 152 × 150 mm was considered. To validate the simulation results, several experiments were conducted using the optimized sheet. Figure 15 illustrates the final geometry of the simple workpiece obtained from the optimized initial blank, which was achieved at a pressure of 24 MPa. Figure 16 shows the optimization stages of the middle-step part obtained at a pressure of 30 MPa. Through the experiments, a reasonable correlation was observed between the results obtained from the simulation and the actual experimental results.

The maximum difference between the two was 8%, indicating a relatively good agreement between them. In performing the optimization process for both the middle-step part and side-step part, by applying the sensitivity correction method, during three stages, the dimensions of the initial sheet were modified, and the final curve closely matched the target curve. During the simulation, the maximum fluid pressure to form the middle-step part and the side-step part was obtained as 35 and 40 MPa, respectively. Figure 17 shows the optimized sheet geometry for three different geometries.

6. 2. The Effects of Optimization Generally, in forming and stretching in the piece, the amount of strain in the radius and rim areas is more than other areas (22). Optimizing the initial sheet shape is a method to reduce thinning in forming. Figure 18 displays the thickness distribution diagrams obtained with the optimized initial

blank for the three investigated parts. It is evident that in the regions corresponding to the first and second steps, the application of fluid pressure results in the contact between the punch and the sheet, thereby minimizing significant thinning throughout the different stages of optimization.

In the three regions corresponding to the punch corner radius, the maximum thinning occurs due to the tensile bending that takes place. However, through the

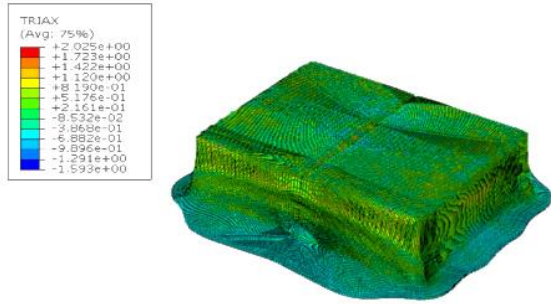


Figure 15. The part formed with optimum initial blank with a step depth of 35 mm and a pressure of 24 MPa and a thickness of 1.5 mm, obtained from simulation

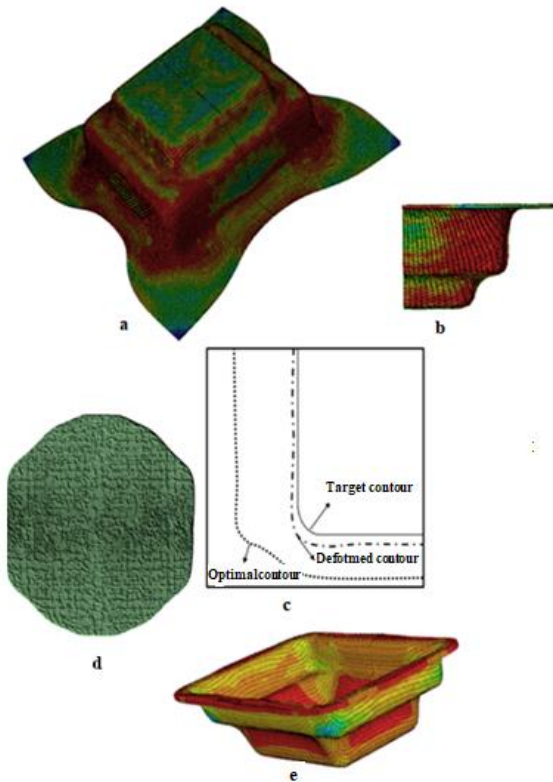


Figure 16. Optimizing stages of the middle-step part with a depth of the lower step of 13 mm, a pressure of 30 MPa, and a thickness of 1.5 mm. a. Formed workpiece with the initial blank, b. Formed workpiece inside view, c. Formed curve diagram and target contour, d. Optimized initial sheet, e. Formed part with optimized sheet, obtained from simulation

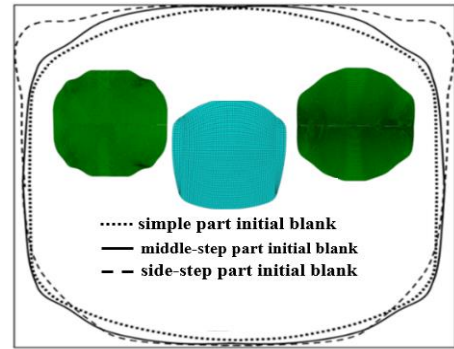
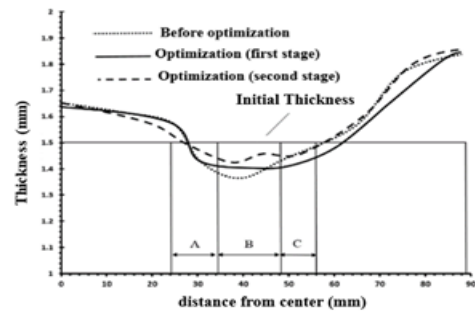
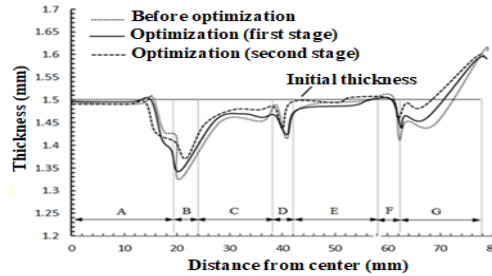


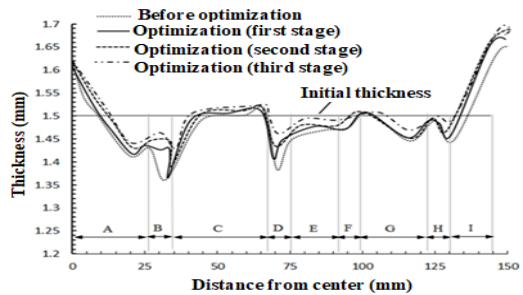
Figure 17. Geometry of the optimized initial blank of the simple part, the middle-step part and the side-step part with optimum pressure and constant initial depth, obtained from simulation



a



b



c

Figure 18. Effect of optimizing the shape of the initial blank on the thickness distribution of: a. Simple workpiece at a depth of 35 mm and a pressure of 24 MPa, b. Middle-step workpiece at the depth of 13 mm at the lower step, and a pressure of 30 MPa. c. Side-step workpiece at the depth of 13 mm at the lower step, and a pressure of 40 MPa, obtained from simulation

optimization of the initial dimensions of the sheet, it is possible to reduce the stress concentrations in the corners. This is achieved by removing sharp corners, resulting in a noticeable decrease in the maximum thinning. Figure 19.a shows the initial and formed sheet metal for the simple part. By performing the optimization stages, thinning in the punch corner radius area in the middle-step and the side-step part was reduced by 4 and 8%, respectively. By performing the optimization stages, the maximum thinning in the mentioned area for the middle-step part and the side-step part is reduced by 3 and 4 percent, respectively. Figure 19.b shows the curve of the initial blank and the shape given in the first and second stages of the simple part optimization.

6. 3. Forming Pressure To investigate the effect of optimization on forming pressure in rectangular and stepped parts, several stages of experimental testing and simulation were performed. Table 2 shows the amount of pressure reduction obtained for different thicknesses and heights of the simple part and the side-step part with the optimal primary sheet at initial pressures of 28 and 40 MPa, respectively. As the diagram shows, the amount of pressure reduction for a simple part has the same upward trend compared to the original sheet before optimization,

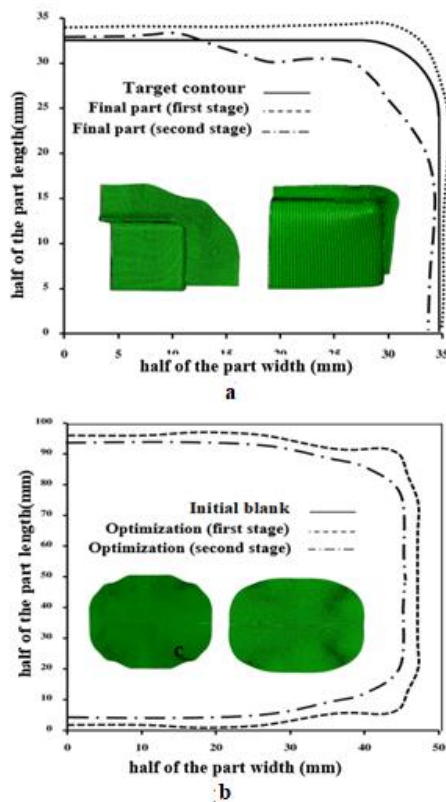


Figure 19. a. The initial blank curve of the simple part, b. The formed blank curve for the simple part in the first and second stages of optimization, obtained from simulation

and from a height of more than 25 mm due to greater elongation in the wall and greater flow of the optimized sheet, it decreases by 16%. By examining the same process for the stepped- part according to the diagrams, it is shown that in the two-step part (in the middle of the step and next to the step) due to the creation of the interface between the first and second steps, with an increase in the height of the lower step due to the need for maximum pressure in the final filling, and the high elongation in the lower step has a lower reduction and will reach a maximum of 13%. Figure 20 shows the thickness reduction of the simple part before and after optimization at a constant pressure of 28 MPa.

TABLE 1. Pressure reduction achieved by optimizing different thicknesses for the simple piece and the side-step part

Simple part					
Depth (mm)	10	20	25	35	Thickness (mm)
Pressure (MPa)	26	24	22	21	1
	26	25	25	23	1.5
	27	26	25	24	2.5
Side-step-part					
Depth (mm)	8	10	13	20	Thickness (mm)
Pressure (MPa)	37	36	35	34	1
	38	37	36	35	1.5
	39	38	37	37	2.5

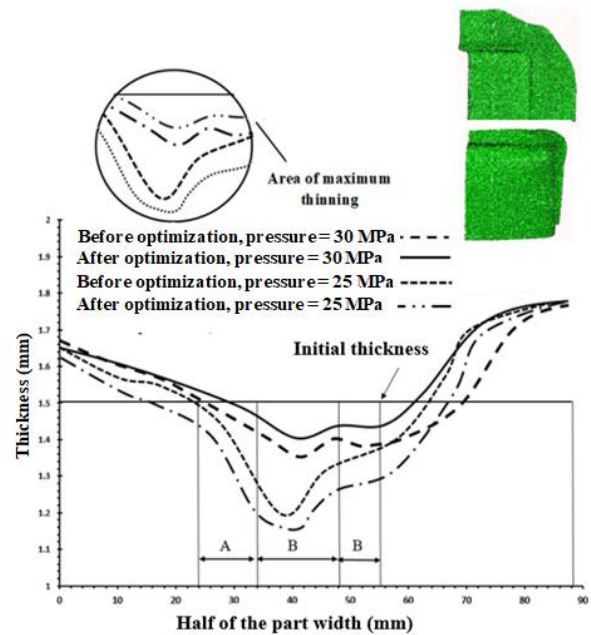


Figure 20. A simple rectangular workpiece obtained with an optimized sheet at a pressure of 32 MPa, a depth of 35 mm and a sheet thickness of 2.5 mm, obtained from simulation

6. 4. Punch Radius To investigate the effects of optimizing the initial blank on determining the minimum radius, the minimum thickness reduction of the part was investigated in different radii at a constant pressure and depth for the part. By optimization, the amount of the minimum selected radius in the part decreases, since the sheet flow and elongation are reduced in the area of the part walls. So that by optimizing the radius of the part from 5 mm to 4 mm, it will remain constant with no change in thinning. Table 3 shows the obtained thickness distribution values for the final thickness of the workpiece before and after optimization.

7. CHANGES IN THE SHAPE OF THE INITIAL BLANK AT DIFFERENT DEPTHS

For each workpiece, the optimal sheet curve changes at different depths. In order to achieve the change process of the initial sheet curve by changing the depth of steps to 15, 20, 25, 30 and 35, simple and two-step rectangular geometries were investigated. Figure 21 shows the zoning of the initial blank to check the material flow. To check the process of changes according to the zoning carried out for three different rectangular geometries, changes in the shape of the initial sheet in the optimization of the simple

and the middle-step parts were examined, which are shown in Figures 22 and 23, respectively. As can be seen, with the change in the shape of the part, the shape of the optimum initial blank will be very different and it is not possible to apply a single optimization process for other geometries and it can't be used for other geometries. So that in the areas of the earring and flange walls in the longitudinal and transverse directions, it needs to change the nodes coordinates (x and y directions) for each geometry. So that, as shown in Figures 24 and 25, if two-step parts have different geometries of the lower step, the flow of material and changes in the coordinates of nodes in the radius and walls are also different. This result was obtained if stepped geometries are considered, depth changes have much more effects on the corners of the optimal sheet and the reason for this is the lack of material flow in the intersection.

With the overview done for the three defined geometries, for the simple rectangular workpiece, due to the initial sheet and the presence of sharp corners, most of the elongation is in the transverse wall. For the side-step workpiece, the material flow is created by removing the nodes in the earring coordinates of the flow in the walls and corners. Three areas: earring area, the transverse wall (the distance between the earrings in the width direction) and the longitudinal wall (the distance between the

TABLE 3. Thickness distribution values obtained for the final thickness of the workpiece before and after optimization

Part type	Destruction before optimization	Destruction after optimization	Destruction before the proper punch radius	Destruction after the proper punch radius
Simple	1.26	1.38	1.24	1.41
side-step	1.23	1.35	1.2	1.29
middle-step	1.24	1.41	1.23	1.35

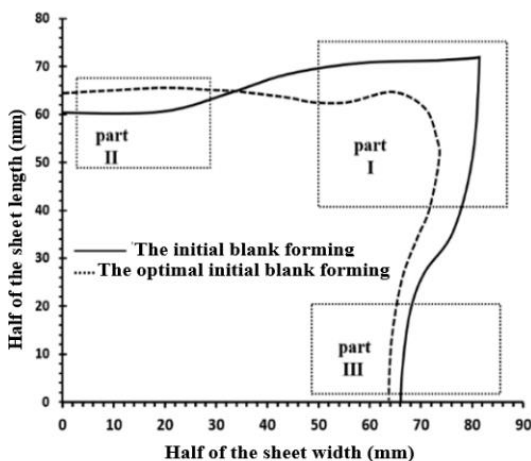


Figure 21. Zoning of the initial sheet to check the material flow, I. Corner radius, II. Transverse wall, and III. Longitudinal wall

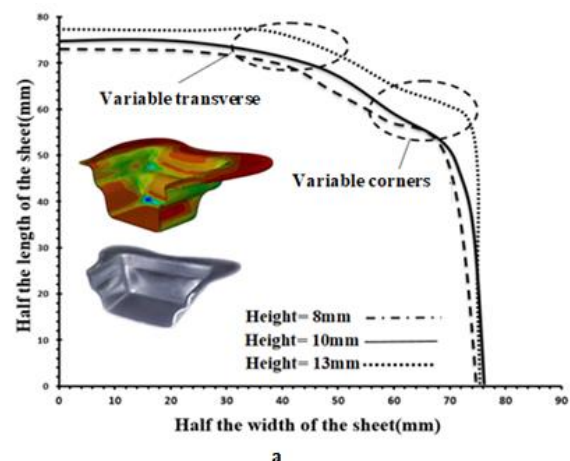


Figure 22. Changes in the shape of the initial sheet in the optimization at different depths of the simple part, obtained from simulation

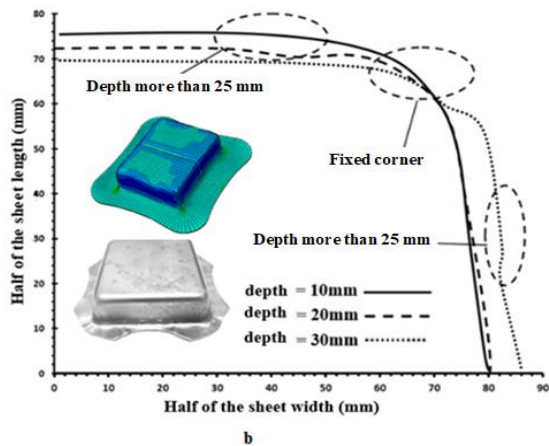


Figure 23. Changes in the shape of the initial sheet in the optimization at different depths of the middle-step part, obtained from simulation

earrings in the length direction) and the process of changes in the material flow in the three mentioned areas at different depths were investigated. At the step depths of 10 and 15 mm with the initial sheet, due to the presence of sharp corners in the sheet and lack of material flow due to the short distances of the transverse wall, because strain in the direction of depth in the transverse wall is more than in other areas, by using the sensitivity method and determining the coordinates of the nodes and removing the sharp corner in the earring area, the flow in the three areas has been balanced and by changing the coordinates of the nodes in the earring area, the optimum shape of the sheet has been achieved. Figure 24 shows the trend of changes in nodes coordinates for the middle-step part.

By conducting repeated experimental tests and validating the experimental and simulation results presented in this research, it was shown that by using the flow chart to determine the pressure and the optimal

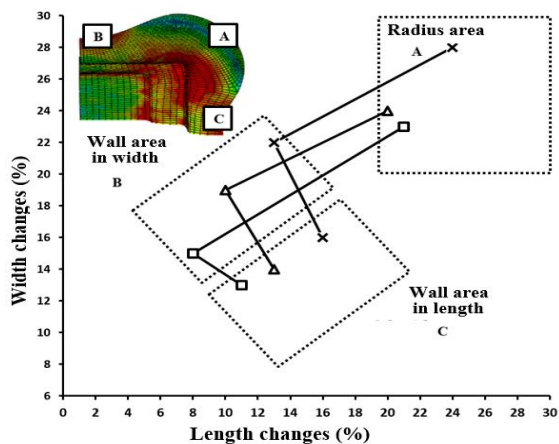


Figure 24. The changes of the node's coordinates in three defined areas of the initial sheet for the middle-step part at a pressure of 24 MPa, obtained from simulation

parameters to form a variety of simple and stepped rectangular parts in different heights and geometries, it is possible to determine the optimal shape of the initial sheet automatically. As an example, a simple rectangular geometry with the dimensions of the initial sheet of 152 x 150 mm and a height of 35 mm was considered. Simulation was performed with Abaqus software to determine the sound part. It was done first by using the flowchart to determine the pressure according to Figure 13, then by defining the rules of the flowchart in Abaqus software and the optimal radius at this height obtained from simulation tests. In the next stage, the simulation was done automatically with computer to determine the shape of the initial sheet. It was performed by defining the rules and relationships of the sensitivity analysis method and coding the rules based on the shape flowchart in Python software, with linking Python and Abaqus software. The first stage of simulation was performed based on the definition of the objective function with the coordinates of the nodes. After simulation and matching the curve with the target curve, if there is deviation from the final node, the software calculates the amount of deviation of the nodes and determines the coordinates of the new nodes based on the sensitivity relationships, rules and coding. The simulation was done again after modifying the initial sheet and was repeated until the curve of the formed sheet matches the target curve so that the optimal initial sheet was obtained in the final stage.

8. AUTOMATION OF DETERMINING THE INITIAL BLANK SHAPE BY COMPUTER

Because all the findings and the upcoming reviews are only related to a sheet sample with a simple rectangular geometry, obviously, its results cannot be generalized to other geometries. Therefore, after examining the simple geometry by experimental and numerical methods and examining the optimal shape changes in different dimensions, to determine the process of changes and ensure the correctness of the process numerically, the process is determined with the help of a flowchart. It is repeated for other different geometries with two steps. The parameters that are emphasized in this part of the research are optimal pressure and corner radius which are analyzed to produce a sound part and the results are presented in a comparative form.

Finally, after predicting the process of changes in the optimum shape of the sheet by changing dimensions of the samples, by linking Python and Abaqus software and the generalization of the sensitivity analysis relationship, the automatic determination of the optimum sheet shape in the process of hydrodynamic deep drawing with radial pressure will be done by the method of metallurgy. So that, hydrodynamic deep drawing operation is done with radial pressure under different tensile limits by

determining the optimal parameters based on the criterion of maximum thinning for each type of geometry and on the other hand by applying the predicted results in the finite element software, the results are compared with the same experimental test conditions. Figure 25 shows the general flowchart of the work stages.

In this article, after examining the effective parameters in compiling the flowchart and comprehensive review the changes in the shape of the initial blank resulted from the change of these parameters as well as manual optimization of the initial sheet shape for different geometries, by determining the proper pressure flowchart for a group of rectangular parts in simple and two-step mode, by using one of the widely used methods of optimization, a flowchart was developed that can be used by Abaqus software and its outputs and its direct linking with Python software. After determining and specifying the desired geometry for forming, it is possible to perform the stages of determining the proper pressure and finally determining the shape of the initial sheet in a closed loop by computer and in the form of a software package. All the stages of checking the outputs, changing the geometric parameters and checking the shape of the initial sheet that matches the optimal target contour, for any depth and geometric shape, can be done by computer through software linking. According to the investigation of the effective parameters in forming and a comprehensive investigation in this regard for simple and two-step parts in different dimensions and depths, the general results of

the change process of each parameter was considered as initial conditions in coding and automation rules. According to the optimization method considered to start the work, the coordinates of all nodes selected on the sheet are determined and considered as initial coordinates for coding. In the following, in order to categorize and determine the process of nodes coordinates changes numerically and to reduce the optimization process error in determining the automatic execution relationships and to determine the validity of the relationships obtained in the automation method by computer, three points in each area considered in the initial blank (corner radius, transverse wall and longitudinal wall) are as A1, A2, A3, B1, B2, B3 and C1, C2, C3 respectively and the changes of nodes coordinates for simple and two-step parts in different dimensions and depths are determined numerically. Figure 26 shows the determination of nodes coordinates in three areas for the simple segment. In Tables 3 and 4, the numerical coordinates obtained for each node are defined according to the points shown in the simple and middle-step parts, respectively. In Figures 27 and 28, the graphs of the changes obtained from these numbers are shown. Also, in Tables 4, 5, 6 and 7, the thickness distribution in the designated areas of the simple and the middle-step workpieces are shown, respectively.

In conducting the research, we were able to numerically obtain the trend of nodes coordinates changes and determine the optimal pressure parameters through

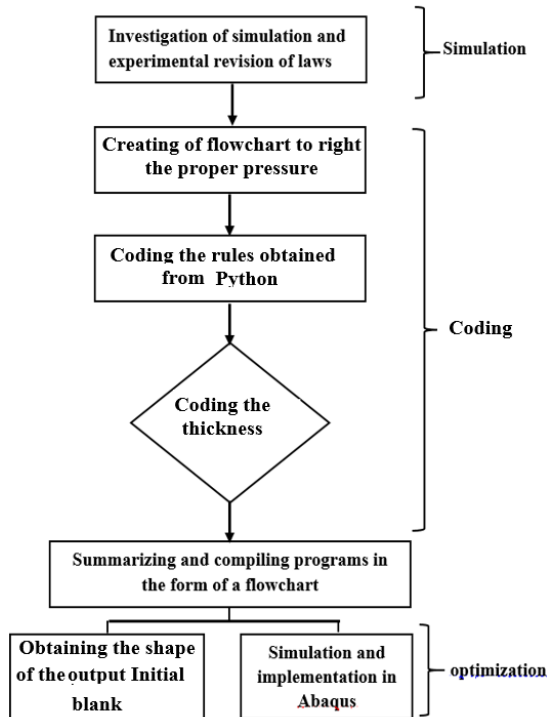


Figure 25. Computer-aided automation process

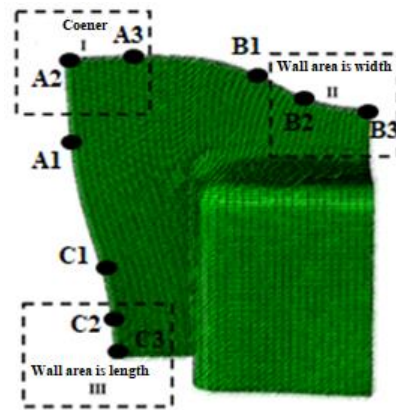


Figure 26. Finding the coordinates of the nodes in the zoning of the simple part in the radius of the punch-A, the transverse wall-B and the longitudinal wall-C

TABLE 4. Thickness distribution values obtained for the final thickness of the simple workpiece

Area	I			II			III		
Node	A1	A2	A3	B1	B2	B3	C1	C2	C3
X	71	73	52	38	31	9	64	57	52
Y	54	69	72	62	54	79	29	21	13

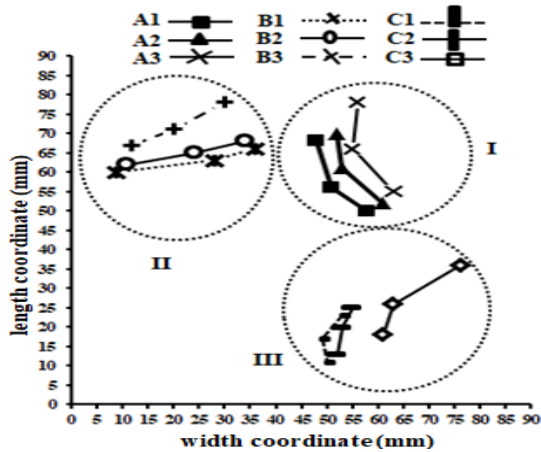


Figure 27. Numerical changes of nodes coordinates in three defined areas of the initial sheet for a simple workpiece at a pressure of 24 MPa and a depth of 35 mm, obtained from simulation

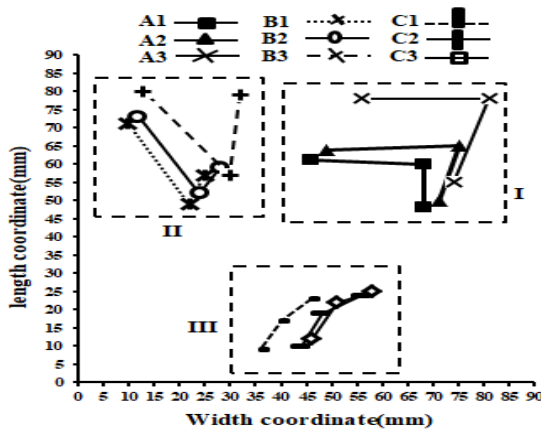


Figure 28. Numerical changes of nodes coordinates in three defined areas of the initial sheet for the middle-step workpiece at a pressure of 30 MPa and a depth of the lower step of 13 mm, obtained from simulation

TABLE 5. Thickness distribution values obtained for the final thickness of the middle-step workpiece

Area	I			II			III		
Node	A1	A2	A3	B1	B2	B3	C1	C2	C3
X	75	79	58	34	28	10	60	52	48
Y	58	71	74	66	58	82	25	19	11

the flowchart, we will determine the proper radius and depth for any simple and rectangular geometry, the parameter rules and the conditions for determining the proper parameters for batch forming of simple and two-step rectangular parts. In order to form any geometry with specific depth and dimensions, the parameters of pressure, radius and approximate dimensions of the initial blank can

TABLE 6. Thickness distribution values obtained for the final thickness of the simple workpiece

Shape	Punch length	Punch width	Punch height	Blank length	Blank width
Simple workpiece	60-75	40-55	H=15-25mm	95	105
			$h \geq 35$ mm	110	125
Simple workpiece	85-110	65-90	H=15-25mm	120	130
			$h \geq 35$ mm	150	152
Simple workpiece	120-160	90-120	H=15-25mm	135	150
			$h \geq 35$ mm	175	185

TABLE 7. Thickness distribution values obtained for the final thickness of the simple workpiece

Shape	Punch length	Punch width	Punch height	Blank length	Blank width
Two-step workpiece	60-75	40-55	$h1 = 15 - 20$ mm, $h1 \leq 13$ mm	135	142
			$h1 = 15 - 20$ mm, $h1 \geq 15$ mm	160	174
Two-step workpiece	85-110	65-90	$h1 = 23 - 27$ mm, $h1 \leq 13$ mm	150	152
			$h1 = 23 - 27$ mm, $h1 \geq 15$ mm	180	195
Two-step workpiece	120-160	90-120	$h1 = 30 - 45$ mm, $h1 \leq 13$ mm	165	180
			$h1 = 23 - 27$ mm, $h1 \geq 15$ mm	195	215

be used to start forming and automatically determine the shape of the initial guessed sheet. To carry out a process to produce the part with the optimal initial sheet shape automatically by computer, based on the general relationships obtained at the beginning, the approximate dimensions of the initial sheet are defined in Abaqus software by defining n points and these points are connected to each other. With the studies done, the rules of the basic relationships of the sensitivity optimization method and the optimal parameters were obtained, which were written in the form of code using the Python programming language. In relations 9 and 10, part of the obtained rules for the parameters and dimensions of the initial blank for simple and two-step parts are shown. Tables 6 and 7 also show the rules for obtaining the dimensions of the initial sheet based on the geometry of the final workpiece and the depth of the drawing. In order to obtain these rules, several stages of simulation were performed to obtain the range of sheet flow changes for each geometry, considering complete forming of the part and the absence of rupture.

Simple part

$$\begin{aligned}
 &h \leq 20mm, r = 4mm \\
 &if \quad h \geq 25mm, r = 6mm, P = 24mpa \quad (9) \\
 &if \quad t \leq 1mm, r = 5mm, P = 22mpa \\
 &if \quad t \geq 1.5mm, r = 5mm, P = 36mpa
 \end{aligned}$$

Two-step geometry

$$\begin{aligned}
 &h1 = 22mm, h2 \leq 15, r = 5mm, P = 40Mpa \\
 &if \quad h \geq 13mm, r = 7mm, P = 42Mpa \quad (10) \\
 &if \quad t \leq 1mm, r = 8mm, P = 34Mpa \\
 &if \quad t \geq 2, r = 6mm, P = 46Mpa
 \end{aligned}$$

Also, the basic relationships of how to categorize the coordinates of the nodes and the sensitivity rules used in coding are shown in relationships 11 to 14. According to the initial relationships of the sensitivity method, n points are considered separately based on the dimensions of the initial sheet and the workpiece in positions of the nodes coordinates in forming and are placed in relation 12 with coding and it is defined as a code based on the sensitivity factor with relation 13 and other defined constants. In relation 14, for each coordinate after forming, the new material point is defined and forming continues until reaching the target point for each target contour of a simple or two-step Workpiece.

$$A_{ij} \begin{matrix} X_j^i \\ Y_j^i \end{matrix}, \quad j = [0....120] \quad (11)$$

$$x_j^{i+1} = x_j^i + \delta N \quad (12)$$

$$S = \frac{x_{j_{i+1}} - x_{j_i}}{x_{j_{i+1}} - x_{j_i}} \quad (13)$$

$$x_j^{i+1} = x_j^i - \varepsilon \delta N \quad (14)$$

According to the dimensions of the final part and using the rules obtained from experimental investigations and repeated simulations, the values of the effective parameters were automatically obtained and used in the simulation. On the other hand, simulation using Abaqus software is also coded with Python programming language and proper parameter values were automatically entered into the software. At the end of each simulation, the coordinates of the initial sheet points were entered into the sensitivity analysis relations and a new simulation with coordinate values was obtained automatically. In this research, by obtaining flowcharts and rules and coding done in Python programming language, the optimum initial blank shape is obtained for each rectangular geometry with different dimensions and depths. With the final review of relationships and rules, the final automation flowchart is shown in Figure 29. In order to

validate the obtained rules and coding, by performing the automatic method of determining the shape of the initial blank and forming the simple and two-step part, the dimensions of the optimum initial blanks and the Formed parts are determined with automatic and computer-aided methods and shown in Figure 30 for simple and two-step (middle-step and side-step) geometries.

In this research, according to the rules for determining the geometric parameters and the pressure flow chart and the basic relationships of the Sensitivity analysis, a solution method was presented. First, each geometry is defined with dimensions and height, then the pressure (P) flowchart (Figure 11) determines the method of setting this parameter in the lines of Abaqus software programs through the call codes. The final appropriate pressure is determined through the criterion of maximum thinning (10) and relations of maximum filling (21) (if step

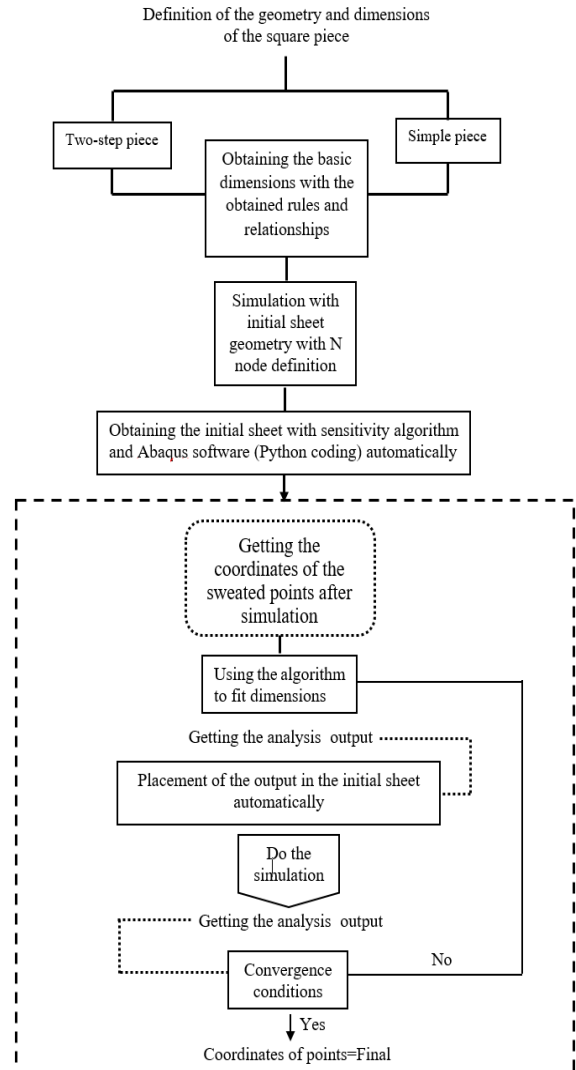


Figure 29. The final flowchart of the initial blank shape automation for all types of rectangular part

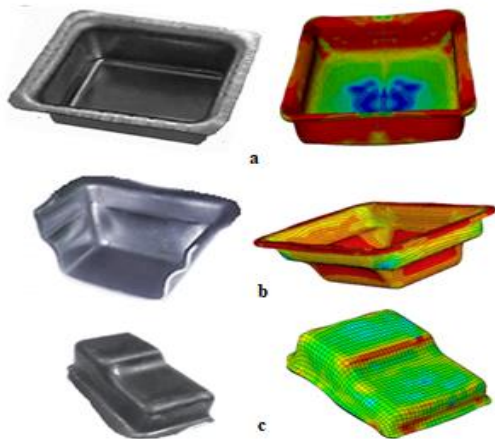


Figure 30. Final Formed parts with optimal initial sheet in simulation and experimental mode, a. Simple part, b. Middle-step part and c. Side-step part

geometry is defined). Then by defining N points or nodes X in the initial sheet and defining the coordinates of the points in the Python software, the simulation of the first step is done with the initial sheet. After checking the coordinates of the shaped sheet $[X_s]$ with the target curve $[X_t]$, the codes defined by Python software of all linked to Abaqus software can determine the deviation nodes from the target curve through the relations of the sensitivity method. Then, the defined codes return to the first line and the simulation is performed until the target curve and the given shape coincide. According to the presented solution method, the amount of deviation of each node is determined with a maximum error of one millimeter. The presented solution method is a new computer-aided method for numerical solution and obtaining the shape of the initial sheet by changing the height and dimensions of various rectangular parts.

9. CONCLUSIONS

The following conclusions have been drawn from the current research:

1. By examining the changes in the height and shape of the part, it was found that for each geometry, the shape of the initial sheet in the area of the transverse, longitudinal and radius walls varies, and the amount of changes in the coordinates of the node relative to the target curve deviates with changes in the geometry and height, and the range of changes of node coordinates of simple and stepped parts.
2. In this research, according to the diversity of rectangular parts geometries, the simulation stages and experimental tests to produce a sound part are reduced, and the ability to define rules in Python and Abaqus software was achieved by providing a flowchart to determine the appropriate pressure.

3. According to the parametric examination of forming of the parts to define the rules, it was found that with the change in the thickness and geometric shape of the final part, the amount of forming pressure and the radius of the punch changes. Moreover, it was investigated that, the amount of changes of these parameters can be determined for different dimensions and thicknesses in the form of rules and relationships and can be defined in the automation software.

4. With the increase of the drawing ratio in the parts, the amount of filling in the stepped parts and the amount of thinning at heights of more than 20 mm decrease up to 8%, due to less strain and lack of flow of the sheet in the radius area of the mold. So, forming pressure should be increased.

5. By performing the optimization stages, with more sheet flow due to the removal of the primary sheet corners, the maximum forming pressure at the beginning of the process and at the end of forming is reduced by 10% and 21%, respectively.

6. In this research, by providing automation rules with the use of a computer and the link of Python and Abaqus software, the initial sheet shape can be obtained by specifying the optimal shaping parameters before performing repeated simulations, and it is possible to save time and money.

10. SUGGESTION FOR OTHERS

The following suggestions are presented at the end of the paper as future works to be done by other researchers to complete this research:

1. Basic optimization methods such as Radius Vector and Taguchi method, and numerical software solution should be implemented to link with Abaqus software for comprehensive application of software and optimization methods.
2. According to the most important circular and polygonal geometries, it is suggested to investigate the automatic optimization procedures for a group of the mentioned geometries to show the generality of the application of this method.
3. According to the application and development of hydroforming methods in the production of sheet parts in the automotive, aerospace and military industries, it is suggested that automatic methods be used to obtain the optimal forming pressure.

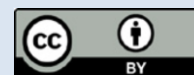
11. REFERENCES

1. Zhang S-H. Developments in hydroforming. *Journal of Materials Processing Technology*. 1999;91(1-3):236-44. <https://doi.org/10.1071/mfreview/1999232>

2. Kocańda A, Sadłowska H. Automotive component development by means of hydroforming. *Archives of Civil and Mechanical Engineering*. 2008;8(3):55-72. <https://doi.org/10.5829/ije.2008.22.02b.30>
3. Lange K, Pöhlandt K. Handbook of metal forming. (No Title). 1985. <https://doi.org/10.1080/09507116.1985.581345>
4. Wong C, Dean T, Lin J. A review of spinning, shear forming and flow forming processes. *International Journal of Machine Tools and Manufacture*. 2003;43(14):1419-35. <https://doi.org/10.1016/j.jengfailanal.2011.114348>
5. Kim J, Kang S-J, Kang B-S. Computational approach to analysis and design of hydroforming process for an automobile lower arm. *Computers & structures*. 2002;80(14-15):1295-304. <https://doi.org/10.1051/mfreview/2002032>
6. Wang H, Gao L, Chen M. Hydrodynamic deep drawing process assisted by radial pressure with inward flowing liquid. *International Journal of Mechanical Sciences*. 2011;53(9):793-9. <https://doi.org/10.1016/j.jengfailanal.2011.114348>
7. Kim T, Yang D-Y, Han S. Numerical modeling of the Multi-stage sheet pair hydroforming process. *Journal of materials processing technology*. 2004;151(1-3):48-53. <https://doi.org/10.1671/mfreview/2004032>
8. Lang L, Danckert J, Nielsen KB. Investigation into hydrodynamic deep drawing assisted by radial pressure: Part I. Experimental observations of the forming process of aluminum alloy. *Journal of Materials Processing Technology*. 2004;148(1):119-31. <https://doi.org/10.1016/j.jengfailanal.2011.114348>
9. Kang B-S, Son B-M, Kim J. A comparative study of stamping and hydroforming processes for an automobile fuel tank using FEM. *International Journal of Machine Tools and Manufacture*. 2004;44(1):87-94. <https://doi.org/10.1016/j.jengfailanal.2011.114348>
10. Zhang S-H, Nielsen KB, Danckert J, Kang D, Lang L. Finite element analysis of the hydromechanical deep-drawing process of tapered rectangular boxes. *Journal of Materials Processing Technology*. 2000;102(1-3):1-8. <https://doi.org/10.1007/s40194-020-00886-3>
11. Wu J, Balendra R, Qin Y. A study on the forming limits of the hydromechanical deep drawing of components with stepped geometries. *Journal of Materials Processing Technology*. 2004;145(2):242-6. <https://doi.org/10.1016/j.jengfailanal.2011.114348>
12. Barlat F, Chung K, Richmond O. Anisotropic plastic potentials for polycrystals and application to the design of optimum blank shapes in sheet forming. *Metallurgical and Materials transactions A*. 1994;25:1209-16. <https://doi.org/10.1007/s40194-009-22886-4>
13. Shim H. Determination of optimal blank shape by the radius vector of boundary nodes. *Proceedings of the Institution of Mechanical Engineers, Part B: Journal of Engineering Manufacture*. 2004;218(9):1099-111. <https://doi.org/10.5829/ije.1994.31.02c.30>
14. Meng B, Wan M, Yuan S, Xu X, Liu J, Huang Z. Influence of cavity pressure on hydrodynamic deep drawing of aluminum alloy rectangular box with wide flange. *International journal of mechanical sciences*. 2013;77:217-26. <https://doi.org/10.1016/j.jengfailanal.2013.102328>
15. Rahmani F, Hashemi SJ, Moslemi Naeini H, Deylami Azodi H. Numerical and experimental study of the efficient parameters on hydromechanical deep drawing of square parts. *Journal of Materials Engineering and Performance*. 2013;22:338-44. <https://doi.org/10.1016/j.jengfailanal.2013.102328>
16. Mousavipoor R, Gorji A, Bakhshi M, Alinejad GM. Experimental and Numerical Study of Effective Parameters in Forming of Double-Stepped Parts and Optimization of the Initial Blank Shape. *Modares Mechanical Engineering*. 2015;15(4). <https://doi.org/10.1016/j.jengfailanal.2013.102328>
17. Luo Y, Luckey S, Friedman P, Peng Y. Development of an advanced superplastic forming process utilizing a mechanical pre-forming operation. *International Journal of Machine Tools and Manufacture*. 2008;48(12-13):1509-18. <https://doi.org/10.1051/mfreview/2015032>
18. Vafaesefat A. Finite element simulation for blank shape optimization in sheet metal forming. *Materials and Manufacturing Processes*. 2011;26(1):93-8. <https://doi.org/10.1016/j.jengfailanal.2013.102328>
19. Blount G, Fischer B. Computerised blank shape prediction for sheet metal components having doubly-curved surfaces. *THE INTERNATIONAL JOURNAL OF PRODUCTION RESEARCH*. 1995;33(4):993-1005. <https://doi.org/10.1016/j.jengfailanal.2013.102328>
20. Xiaojing L, Yongchao X, Shijian Y. Effects of loading paths on hydrodynamic deep drawing with independent radial hydraulic pressure of aluminum alloy based on numerical simulation. *Journal of Materials Sciences and Technology*. 2008;24(03):395. <https://doi.org/10.1007/s40194-009-22886-4>
21. Bakhshi M, Hosseinipour SJ, Gorji A. The Study of effective parameters in hydroforming of fuel cell metallic bipolar plates with parallel serpentine flow field. *Modares Mechanical Engineering*. 2014;14(8):17-27. <https://doi.org/10.1007/s40194-009-22886-4>
22. Panahi Leavoli R, Gorji H, Bakhshi-Jooybari M, Mirnia M. Investigation on formability of tailor-welded blanks in incremental forming. *International Journal of Engineering, Transactions B: Applications*. 2020;33(5):906-15. <https://doi.org/10.5829/ije.2020.33.05b.23>

COPYRIGHTS

©2024 The author(s). This is an open access article distributed under the terms of the Creative Commons Attribution (CC BY 4.0), which permits unrestricted use, distribution, and reproduction in any medium, as long as the original authors and source are cited. No permission is required from the authors or the publishers.



Persian Abstract

چکیده

در این تحقیق از روشی ابتکاری برای بدست آوردن شکل ورق اولیه در شکل دهی هندسه های مختلف مستطیلی استفاده شده است تا بتوانیم قوانینی را به دست آوریم که به طور خودکار شکل ورق اولیه بهینه را در ارتفاعات مختلف تعیین نمود. از روش آنالیز حساسیت برای بهینه سازی و از نرم افزار پایتون برای لینک با نرم افزار آباکوس استفاده گردید. با بررسی پارامترهای هندسی و فشار شکل دهی، فلوچارت تعیین فشار مناسب ارائه گردید. با بررسی تغییرات ارتفاع در هندسه های مختلف مشخص گردید که بهینه سازی سبب کاهش فشار بیشینه و حداکثر شعاع سنبه می گردد که به ترتیب 4 و 8 درصد بدست آمد. مشخص گردید که اختلاف اندازه اضلاع طولی و عرضی مقطع قطعه تاثیر مستقیم بر روی تغییرات مختصات گره برای انطباق با منحنی هدف دارد و تعداد مراحل بهینه سازی را کاهش می دهد. از نتایج بدست آمده نشان داده شد که با خودکار سازی و تعیین فلوچارت فشار، بدون تکرار در مراحل بهینه سازی و تست های تجربی مکرر، با حداقل مراحل بهینه سازی می توان شکل ورق اولیه را تعیین نمود و از دور بری جلوگیری نمود.
